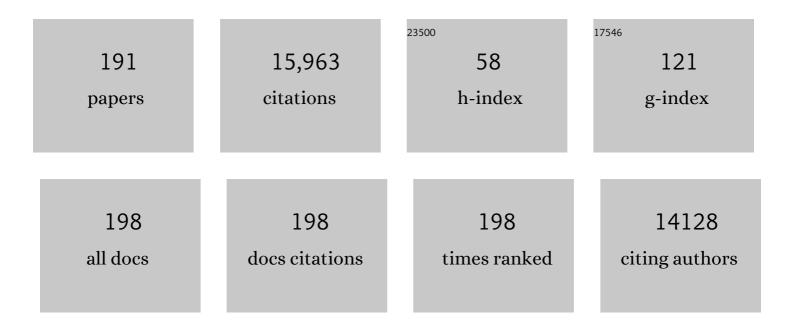
List of Publications by Year in descending order

Source: https://exaly.com/author-pdf/6444273/publications.pdf Version: 2024-02-01



#	Article	lF	CITATIONS
1	Thermally stable single-atom platinum-on-ceria catalysts via atom trapping. Science, 2016, 353, 150-154.	6.0	1,487
2	Activation of surface lattice oxygen in single-atom Pt/CeO <sub>2</sub> for low-temperature CO oxidation. Science, 2017, 358, 1419-1423.	6.0	1,114
3	Catalytic fast pyrolysis of lignocellulosic biomass. Chemical Society Reviews, 2014, 43, 7594-7623.	18.7	864
4	Catalysis with Two-Dimensional Materials Confining Single Atoms: Concept, Design, and Applications. Chemical Reviews, 2019, 119, 1806-1854.	23.0	745
5	Recent Advances in Hydrotreating of Pyrolysis Bio-Oil and Its Oxygen-Containing Model Compounds. ACS Catalysis, 2013, 3, 1047-1070.	5.5	585
6	Recent Advances in Catalytic Conversion of Ethanol to Chemicals. ACS Catalysis, 2014, 4, 1078-1090.	5.5	494
7	Recent advance in MXenes: A promising 2D material for catalysis, sensor and chemical adsorption. Coordination Chemistry Reviews, 2017, 352, 306-327.	9.5	484
8	Carbon-supported bimetallic Pd–Fe catalysts for vapor-phase hydrodeoxygenation of guaiacol. Journal of Catalysis, 2013, 306, 47-57.	3.1	384
9	Review of Developments in Portable Hydrogen Production Using Microreactor Technology. Chemical Reviews, 2004, 104, 4767-4790.	23.0	354
10	Bimetallic catalysts for hydrogen generation. Chemical Society Reviews, 2012, 41, 7994.	18.7	309
11	Tuning Pt-CeO2 interactions by high-temperature vapor-phase synthesis for improved reducibility of lattice oxygen. Nature Communications, 2019, 10, 1358.	5.8	302
12	Toward Rational Design of Cu/SSZ-13 Selective Catalytic Reduction Catalysts: Implications from Atomic-Level Understanding of Hydrothermal Stability. ACS Catalysis, 2017, 7, 8214-8227.	5.5	278
13	Steam reforming of methanol over highly active Pd/ZnO catalyst. Catalysis Today, 2002, 77, 79-88.	2.2	245
14	Stabilizing High Metal Loadings of Thermally Stable Platinum Single Atoms on an Industrial Catalyst Support. ACS Catalysis, 2019, 9, 3978-3990.	5.5	233
15	Direct Conversion of Bio-ethanol to Isobutene on Nanosized Zn <sub><i>x</i></sub> Zr <sub><i>y</i></sub> O <sub><i>z</i></sub> Mixed Oxides with Balanced Acid–Base Sites. Journal of the American Chemical Society, 2011, 133, 11096-11099.	6.6	225
16	Nitrogenâ€Doped Porous Carbon Supported Nonprecious Metal Singleâ€Atom Electrocatalysts: from Synthesis to Application. Small Methods, 2019, 3, 1900159.	4.6	218
17	Fabrication and thermal stability of NH 4 HF 2 -etched Ti 3 C 2 MXene. Ceramics International, 2017, 43, 6322-6328.	2.3	208
18	Low-Temperature Pd/Zeolite Passive NO <sub><i>x</i></sub> Adsorbers: Structure, Performance, and Adsorption Chemistry. Journal of Physical Chemistry C, 2017, 121, 15793-15803.	1.5	178

#	Article	IF	CITATIONS
19	Synergistic Catalysis between Pd and Fe in Gas Phase Hydrodeoxygenation of <i>m</i> -Cresol. ACS Catalysis, 2014, 4, 3335-3345.	5.5	173
20	Stable platinum nanoparticles on specific MgAl2O4 spinel facets at high temperatures in oxidizing atmospheres. Nature Communications, 2013, 4, 2481.	5.8	166
21	Visualizing H <sub>2</sub> O molecules reacting at TiO <sub>2</sub> active sites with transmission electron microscopy. Science, 2020, 367, 428-430.	6.0	149
22	Catalysts for Steam Reforming of Bio-oil: A Review. Industrial & Engineering Chemistry Research, 2017, 56, 4627-4637.	1.8	139
23	Recent advances in the selective catalytic hydrodeoxygenation of lignin-derived oxygenates to arenes. Green Chemistry, 2020, 22, 1072-1098.	4.6	130
24	Achieving Atomic Dispersion of Highly Loaded Transition Metals in Smallâ€Pore Zeolite SSZâ€13: Highâ€Capacity and Highâ€Efficiency Lowâ€Temperature CO and Passive NO <sub><i>x</i></sub> Adsorbers. Angewandte Chemie - International Edition, 2018, 57, 16672-16677.	7.2	129
25	Thermally Stable Singleâ€Atom Heterogeneous Catalysts. Advanced Materials, 2021, 33, e2004319.	11.1	127
26	Elucidation of the Active Sites in Single-Atom Pd <sub>1</sub> /CeO <sub>2</sub> Catalysts for Low-Temperature CO Oxidation. ACS Catalysis, 2020, 10, 11356-11364.	5.5	123
27	Genesis and Stability of Hydronium Ions in Zeolite Channels. Journal of the American Chemical Society, 2019, 141, 3444-3455.	6.6	119
28	Phenol Deoxygenation Mechanisms on Fe(110) and Pd(111). ACS Catalysis, 2015, 5, 523-536.	5.5	116
29	Enhanced Fe <sub>2</sub> O <sub>3</sub> Reducibility via Surface Modification with Pd: Characterizing the Synergy within Pd/Fe Catalysts for Hydrodeoxygenation Reactions. ACS Catalysis, 2014, 4, 3381-3392.	5.5	114
30	Toward efficient single-atom catalysts for renewable fuels and chemicals production from biomass and CO2. Applied Catalysis B: Environmental, 2021, 292, 120162.	10.8	114
31	Intensified Fischer–Tropsch synthesis process with microchannel catalytic reactors. Catalysis Today, 2009, 140, 149-156.	2.2	112
32	Hydrothermal catalytic deoxygenation of palmitic acid over nickel catalyst. Fuel, 2016, 166, 302-308.	3.4	110
33	Role of Active Phase in Fischer–Tropsch Synthesis: Experimental Evidence of CO Activation over Single-Phase Cobalt Catalysts. ACS Catalysis, 2018, 8, 7787-7798.	5.5	110
34	Real-Time Observation of Reconstruction Dynamics on TiO <sub>2</sub> (001) Surface under Oxygen via an Environmental Transmission Electron Microscope. Nano Letters, 2016, 16, 132-137.	4.5	109
35	A review on ex situ catalytic fast pyrolysis of biomass. Frontiers of Chemical Science and Engineering, 2014, 8, 280-294.	2.3	103
36	Elucidation of Active Sites for CH <sub>4</sub> Catalytic Oxidation over Pd/CeO <sub>2</sub> Via Tailoring Metal–Support Interactions. ACS Catalysis, 2021, 11, 5666-5677.	5.5	103

#	Article	IF	CITATIONS
37	Sub-micron Cu/SSZ-13: Synthesis and application as selective catalytic reduction (SCR) catalysts. Applied Catalysis B: Environmental, 2017, 201, 461-469.	10.8	101
38	Molecular Level Understanding of How Oxygen and Carbon Monoxide Improve NO <sub><i>x</i></sub> Storage in Palladium/SSZ-13 Passive NO <sub><i>x</i></sub> Adsorbers: The Role of NO <sup>+</sup> and Pd(II)(CO)(NO) Species. Journal of Physical Chemistry C, 2018, 122, 10820-10827.	1.5	101
39	Influence of ZnO Facets on Pd/ZnO Catalysts for Methanol Steam Reforming. ACS Catalysis, 2014, 4, 2379-2386.	5.5	99
40	Unraveling the mysterious failure of Cu/SAPO-34 selective catalytic reduction catalysts. Nature Communications, 2019, 10, 1137.	5.8	99
41	Catalytic Roles of Co <sup>0</sup> and Co <sup>2+</sup> during Steam Reforming of Ethanol on Co/MgO Catalysts. ACS Catalysis, 2011, 1, 279-286.	5.5	98
42	Effect of Oxygen Defects on the Catalytic Performance of VO <sub><i>x</i></sub> /CeO <sub>2</sub> Catalysts for Oxidative Dehydrogenation of Methanol. ACS Catalysis, 2015, 5, 3006-3012.	5.5	96
43	Mechanism by which Tungsten Oxide Promotes the Activity of Supported V <sub>2</sub> O <sub>5</sub> /TiO <sub>2</sub> Catalysts for NO <sub><i>X</i></sub> Abatement: Structural Effects Revealed by <sup>51</sup> V MAS NMR Spectroscopy. Angewandte Chemie - International Edition. 2019. 58. 12609-12616.	7.2	96
44	Methanol steam reforming over Pd/ZnO: Catalyst preparation and pretreatment studies. Fuel Processing Technology, 2003, 83, 193-201.	3.7	93
45	Low-Temperature Methane Oxidation for Efficient Emission Control in Natural Gas Vehicles: Pd and Beyond. ACS Catalysis, 2020, 10, 14304-14314.	5.5	93
46	Correlating DFT Calculations with CO Oxidation Reactivity on Ga-Doped Pt/CeO <sub>2</sub> Single-Atom Catalysts. Journal of Physical Chemistry C, 2018, 122, 22460-22468.	1.5	91
47	Engineering catalyst supports to stabilize PdOx two-dimensional rafts for water-tolerant methane oxidation. Nature Catalysis, 2021, 4, 830-839.	16.1	86
48	Tailoring the Local Environment of Platinum in Singleâ€Atom Pt <sub>1</sub> /CeO <sub>2</sub> Catalysts for Robust Lowâ€Temperature CO Oxidation. Angewandte Chemie - International Edition, 2021, 60, 26054-26062.	7.2	84
49	Palladium/Beta zeolite passive NOx adsorbers (PNA): Clarification of PNA chemistry and the effects of CO and zeolite crystallite size on PNA performance. Applied Catalysis A: General, 2019, 569, 141-148.	2.2	81
50	Propane oxidative dehydrogenation over highly selective hexagonal boron nitride catalysts: The role of oxidative coupling of methyl. Science Advances, 2019, 5, eaav8063.	4.7	80
51	Recent advances in hybrid metal oxide–zeolite catalysts for low-temperature selective catalytic reduction of NOx by ammonia. Applied Catalysis B: Environmental, 2021, 291, 120054.	10.8	78
52	A comparative study between Co and Rh for steam reforming of ethanol. Applied Catalysis B: Environmental, 2010, 96, 441-448.	10.8	77
53	Recent Progresses on Structural Reconstruction of Nanosized Metal Catalysts via Controlled-Atmosphere Transmission Electron Microscopy: A Review. ACS Catalysis, 2020, 10, 14419-14450.	5.5	71
54	CdS/ZnO: A Multipronged Approach for Efficient Reduction of Carbon Dioxide under Visible Light Irradiation. ACS Sustainable Chemistry and Engineering, 2020, 8, 5270-5277.	3.2	70

#	Article	IF	CITATIONS
55	New insights into reaction mechanisms of ethanol steam reforming on Co–ZrO2. Applied Catalysis B: Environmental, 2015, 162, 141-148.	10.8	67
56	Stabilization of Super Electrophilic Pd <sup>+2</sup> Cations in Small-Pore SSZ-13 Zeolite. Journal of Physical Chemistry C, 2020, 124, 309-321.	1.5	67
57	Probing Active-Site Relocation in Cu/SSZ-13 SCR Catalysts during Hydrothermal Aging by In Situ EPR Spectroscopy, Kinetics Studies, and DFT Calculations. ACS Catalysis, 2020, 10, 9410-9419.	5.5	64
58	Hierarchical Echinus-like Cu-MFI Catalysts for Ethanol Dehydrogenation. ACS Catalysis, 2020, 10, 13624-13629.	5.5	63
59	Supported metal catalysts for alcohol/sugar alcohol steam reforming. Dalton Transactions, 2014, 43, 11782.	1.6	60
60	Sorption-enhanced synthetic natural gas (SNG) production from syngas: A novel process combining CO methanation, water-gas shift, and CO2 capture. Applied Catalysis B: Environmental, 2014, 144, 223-232.	10.8	59
61	Revisiting effects of alkali metal and alkaline earth co-cation additives to Cu/SSZ-13 selective catalytic reduction catalysts. Journal of Catalysis, 2019, 378, 363-375.	3.1	59
62	Direct conversion of methane to formaldehyde and CO on B2O3 catalysts. Nature Communications, 2020, 11, 5693.	5.8	59
63	Carbon vacancy defect-activated Pt cluster for hydrogen generation. Journal of Materials Chemistry A, 2019, 7, 15364-15370.	5.2	57
64	The superior hydrothermal stability of Pd/SSZ-39 in low temperature passive NOx adsorption (PNA) and methane combustion. Applied Catalysis B: Environmental, 2021, 280, 119449.	10.8	56
65	Mechanistic insight into the passive NOx adsorption in the highly dispersed Pd/HBEA zeolite. Applied Catalysis A: General, 2019, 569, 181-189.	2.2	55
66	Direct Coupling of Thermo―and Photocatalysis for Conversion of CO <sub>2</sub> –H <sub>2</sub> O into Fuels. ChemSusChem, 2017, 10, 4709-4714.	3.6	53
67	Controllable in Situ Surface Restructuring of Cu Catalysts and Remarkable Enhancement of Their Catalytic Activity. ACS Catalysis, 2019, 9, 2213-2221.	5.5	53
68	Controlled Synthesis of Cu <sup>0</sup> /Cu <sub>2</sub> O for Efficient Photothermal Catalytic Conversion of CO <sub>2</sub> and H <sub>2</sub> O. ACS Sustainable Chemistry and Engineering, 2021, 9, 1754-1761.	3.2	53
69	Adsorption of phenol on Fe (110) and Pd (111) from first principles. Surface Science, 2014, 630, 244-253.	0.8	52
70	Investigation of the Structure and Active Sites of TiO <sub>2</sub> Nanorod Supported VO <sub><i>x</i></sub> Catalysts by High-Field and Fast-Spinning <sup>51</sup> V MAS NMR. ACS Catalysis, 2015, 5, 3945-3952.	5.5	51
71	Economizing on Precious Metals in Threeâ€Way Catalysts: Thermally Stable and Highly Active Singleâ€Atom Rhodium on Ceria for NO Abatement under Dry and Industrially Relevant Conditions**. Angewandte Chemie - International Edition, 2021, 60, 391-398.	7.2	51
72	Mechanistic Effects of Water on the Fe-Catalyzed Hydrodeoxygenation of Phenol. The Role of BrÃ,nsted Acid Sites. ACS Catalysis, 2018, 8, 2200-2208.	5.5	50

#	Article	IF	CITATIONS
73	Variable Temperature and Pressure Operando MAS NMR for Catalysis Science and Related Materials. Accounts of Chemical Research, 2020, 53, 611-619.	7.6	48
74	High field 27Al MAS NMR and TPD studies of active sites in ethanol dehydration using thermally treated transitional aluminas as catalysts. Journal of Catalysis, 2016, 336, 85-93.	3.1	47
75	Atom trapping: a novel approach to generate thermally stable and regenerable single-atom catalysts. National Science Review, 2018, 5, 630-632.	4.6	47
76	Catalytic reactivity of face centered cubic PdZnα for the steam reforming of methanol. Journal of Catalysis, 2012, 291, 44-54.	3.1	46
77	Tailoring the Adsorption of Benzene on PdFe Surfaces: A Density Functional Theory Study. Journal of Physical Chemistry C, 2013, 117, 24317-24328.	1.5	45
78	Mechanism by which Tungsten Oxide Promotes the Activity of Supported V <sub>2</sub> O <sub>5</sub> /TiO <sub>2</sub> Catalysts for NO <sub><i>X</i></sub> Abatement: Structural Effects Revealed by <sup>51</sup> V MAS NMR Spectroscopy. Angewandte Chemie, 2019, 131, 12739-12746.	1.6	45
79	Perspective on Catalytic Hydrodeoxygenation of Biomass Pyrolysis Oils: Essential Roles of Fe-Based Catalysts. Catalysis Letters, 2016, 146, 1621-1633.	1.4	42
80	Enhancement of high-temperature selectivity on Cu-SSZ-13 towards NH3-SCR reaction from highly dispersed ZrO2. Applied Catalysis B: Environmental, 2020, 263, 118359.	10.8	42
81	In Situ STEM Determination of the Atomic Structure and Reconstruction Mechanism of the TiO <sub>2</sub> (001) (1 × 4) Surface. Chemistry of Materials, 2017, 29, 3189-3194.	3.2	40
82	Hydrothermal Catalytic Deoxygenation of Fatty Acid and Bio-oil with In Situ H <sub>2</sub> . ACS Sustainable Chemistry and Engineering, 2018, 6, 4521-4530.	3.2	40
83	Influences of Na+ co-cation on the structure and performance of Cu/SSZ-13 selective catalytic reduction catalysts. Catalysis Today, 2020, 339, 233-240.	2.2	40
84	Investigation of Silica-Supported Vanadium Oxide Catalysts by High-Field <sup>51</sup> V Magic-Angle Spinning NMR. Journal of Physical Chemistry C, 2017, 121, 6246-6254.	1.5	39
85	Inhibition of AlF <sub>3</sub> ·3H <sub>2</sub> O Impurity Formation in Ti <sub>3</sub> C <sub>2</sub> T <sub><i>x</i> </sub> MXene Synthesis under a Unique CoF <sub><i>x</i> </sub> /HCl Etching Environment. ACS Applied Energy Materials, 2019, 2, 8145-8152.	2.5	39
86	Tuning Ni/Al Ratio to Enhance Pseudocapacitive Charge Storage Properties of Nickel–Aluminum Layered Double Hydroxide. Advanced Electronic Materials, 2019, 5, 1900215.	2.6	39
87	Palladium/Zeolite Low Temperature Passive NOx Adsorbers (PNA): Structure-Adsorption Property Relationships for Hydrothermally Aged PNA Materials. Emission Control Science and Technology, 2020, 6, 126-138.	0.8	38
88	Atomically Dispersed Dopants for Stabilizing Ceria Surface Area. Applied Catalysis B: Environmental, 2021, 284, 119722.	10.8	37
89	Onset of High Methane Combustion Rates over Supported Palladium Catalysts: From Isolated Pd Cations to PdO Nanoparticles. Jacs Au, 2021, 1, 396-408.	3.6	37
90	Hydrogen spillover assisted by oxygenate molecules over nonreducible oxides. Nature Communications, 2022, 13, 1457.	5.8	37

#	Article	IF	CITATIONS
91	Oxidation of ethanol to acetaldehyde over Na-promoted vanadium oxide catalysts. Applied Catalysis A: General, 2007, 332, 263-272.	2.2	36
92	The Effect of Zinc Addition on the Oxidation State of Cobalt in Co/ZrO <sub>2</sub> Catalysts. ChemSusChem, 2011, 4, 1679-1684.	3.6	36
93	Adsorption of guaiacol on Fe (110) and Pd (111) from first principles. Surface Science, 2016, 648, 227-235.	0.8	36
94	Stabilization of Iron-Based Catalysts against Oxidation: An <i>In Situ</i> Ambient-Pressure X-ray Photoelectron Spectroscopy (AP-XPS) Study. ACS Catalysis, 2017, 7, 3639-3643.	5.5	36
95	Minimizing the Formation of Coke and Methane on Co Nanoparticles in Steam Reforming of Biomassâ€Đerived Oxygenates. ChemCatChem, 2013, 5, 1299-1303.	1.8	34
96	Achieving Atomic Dispersion of Highly Loaded Transition Metals in Smallâ€Pore Zeolite SSZâ€13: Highâ€Capacity and Highâ€Efficiency Lowâ€Temperature CO and Passive NO <sub><i>x</i></sub> Adsorbers. Angewandte Chemie, 2018, 130, 16914-16919.	1.6	34
97	Single-Step Conversion of Ethanol to <i>n</i> -Butene over Ag-ZrO <sub>2</sub> /SiO <sub>2</sub> Catalysts. ACS Catalysis, 2020, 10, 10602-10613.	5.5	34
98	Aerosol-Derived Bimetallic Alloy Powders: Bridging the Gap. Journal of Physical Chemistry C, 2010, 114, 17181-17190.	1.5	33
99	Ethanol Partial Oxidation over VO <sub><i>x</i></sub> /TiO <sub>2</sub> Catalysts: The Role of Titania Surface Oxygen on Vanadia Reoxidation in the Mars–van Krevelen Mechanism. ACS Catalysis, 2018, 8, 4681-4693.	5.5	33
100	Controlling the Oxidation State of Fe-Based Catalysts through Nitrogen Doping toward the Hydrodeoxygenation of <i>m</i> -Cresol. ACS Catalysis, 2020, 10, 7884-7893.	5.5	32
101	Single-Facet Dominant Anatase TiO <sub>2</sub> (101) and (001) Model Catalysts to Elucidate the Active Sites for Alkanol Dehydration. ACS Catalysis, 2020, 10, 4268-4279.	5.5	32
102	Selective catalytic reduction of NOx with NH3 over Ce-Mn oxide and Cu-SSZ-13 composite catalysts – Low temperature enhancement. Applied Catalysis B: Environmental, 2022, 316, 121522.	10.8	32
103	One-Pot Production of Lactic Acid from Acetol over Dealuminated Sn-Beta Supported Gold Catalyst. ACS Catalysis, 2017, 7, 6038-6047.	5.5	31
104	Conversion of syngas to methanol and DME on highly selective Pd/ZnAl2O4 catalyst. Journal of Energy Chemistry, 2021, 58, 564-572.	7.1	31
105	Liquid-phase hydrodeoxygenation of lignin-derived phenolics on Pd/Fe: A mechanistic study. Catalysis Today, 2020, 339, 305-311.	2.2	29
106	High-Field One-Dimensional and Two-Dimensional <sup>27</sup> Al Magic-Angle Spinning Nuclear Magnetic Resonance Study of Î,-, Î-, and γ-Al <sub>2</sub> O <sub>3</sub> Dominated Aluminum Oxides: Toward Understanding the Al Sites in γ-Al <sub>2</sub> O <sub>3</sub> . ACS Omega, 2021, 6, 4090-4099.	1.6	29
107	Nanocrystalline Anatase Titania-Supported Vanadia Catalysts: Facet-Dependent Structure of Vanadia. Journal of Physical Chemistry C, 2015, 119, 15094-15102.	1.5	28
108	High CO2 Selectivity of ZnO Powder Catalysts for Methanol Steam Reforming. Journal of Physical Chemistry C, 2013, 117, 6493-6503.	1.5	27

#	Article	IF	CITATIONS
109	Singleâ€atom Automobile Exhaust Catalysts. ChemNanoMat, 2020, 6, 1659-1682.	1.5	27
110	Investigating the Surface Structure of γ-Al <sub>2</sub> O <sub>3</sub> Supported WO <sub>X</sub> Catalysts by High Field <sup>27</sup> Al MAS NMR and Electronic Structure Calculations. Journal of Physical Chemistry C, 2016, 120, 23093-23103.	1.5	26
111	Elucidation of Active Sites in Aldol Condensation of Acetone over Single-Facet Dominant Anatase TiO <sub>2</sub> (101) and (001) Catalysts. Jacs Au, 2021, 1, 41-52.	3.6	26
112	Effect of Sodium on the Catalytic Properties of VO <sub><i>x</i></sub> /CeO <sub>2</sub> Catalysts for Oxidative Dehydrogenation of Methanol. Journal of Physical Chemistry C, 2013, 117, 5722-5729.	1.5	25
113	The effect of ZnO addition on Co/C catalyst for vapor and aqueous phase reforming of ethanol. Catalysis Today, 2014, 233, 38-45.	2.2	25
114	Distinct Role of Surface Hydroxyls in Single-Atom Pt <sub>1</sub> /CeO <sub>2</sub> Catalyst for Room-Temperature Formaldehyde Oxidation: Acid–Base Versus Redox. Jacs Au, 2022, 2, 1651-1660.	3.6	25
115	Low-temperature aqueous-phase reforming of ethanol on bimetallic PdZn catalysts. Catalysis Science and Technology, 2015, 5, 254-263.	2.1	24
116	Nitrogen-doped flower-like porous carbon materials directed by in situ hydrolysed MgO: Promising support for Ru nanoparticles in catalytic hydrogenations. Nano Research, 2016, 9, 3129-3140.	5.8	24
117	Effect of Water on Ethanol Conversion over ZnO. Topics in Catalysis, 2016, 59, 37-45.	1.3	24
118	Palladium/Ferrierite versus Palladium/SSZâ€13 Passive NOx Adsorbers: Adsorbateâ€Controlled Location of Atomically Dispersed Palladium(II) in Ferrierite Determines High Activity and Stability**. Angewandte Chemie - International Edition, 2022, 61, .	7.2	24
119	Probing Acid–Base Properties of Anatase TiO <sub>2</sub> Nanoparticles with Dominant {001} and {101} Facets Using Methanol Chemisorption and Surface Reactions. Journal of Physical Chemistry C, 2021, 125, 3988-4000.	1.5	23
120	Vapor-phase self-assembly for generating thermally stable single-atom catalysts. CheM, 2022, 8, 731-748.	5.8	23
121	Coordination environment of active sites and their effect on catalytic performance of heterogeneous catalysts. Chinese Journal of Catalysis, 2022, 43, 928-955.	6.9	23
122	Effect of ZnO facet on ethanol steam reforming over Co/ZnO. Catalysis Communications, 2016, 73, 93-97.	1.6	22
123	Cu-Exchanged CHA-Type Zeolite from Organic Template-Free Synthesis: An Effective Catalyst for NH <sub>3</sub> -SCR. Industrial & Engineering Chemistry Research, 2020, 59, 7375-7382.	1.8	22
124	Elucidating the Role of CO in the NO Storage Mechanism on Pd/SSZ-13 with <i>in Situ</i> DRIFTS. Journal of Physical Chemistry C, 2022, 126, 1439-1449.	1.5	22
125	Shapeâ€Dependent Performance of Cu/Cu <sub>2</sub> O for Photocatalytic Reduction of CO <sub>2</sub> 2. ChemSusChem, 2022, 15, .	3.6	22
126	Conversion of ethanol to 1,3–butadiene over Ag–ZrO2/SiO2 catalysts: The role of surface interfaces. Journal of Energy Chemistry, 2021, 54, 7-15.	7.1	21

#	Article	IF	CITATIONS
127	A large sample volume magic angle spinning nuclear magnetic resonance probe for in situ investigations with constant flow of reactants. Physical Chemistry Chemical Physics, 2012, 14, 2137-2143.	1.3	20
128	Catalytic activation of ethylene C–H bonds on uniform d <sup>8</sup> Ir( <scp>i</scp> ) and Ni( <scp>ii</scp> ) cations in zeolites: toward molecular level understanding of ethylene polymerization on heterogeneous catalysts. Catalysis Science and Technology, 2019, 9, 6570-6576.	2.1	20
129	Quantitative Cu Counting Methodologies for Cu/SSZ-13 Selective Catalytic Reduction Catalysts by Electron Paramagnetic Resonance Spectroscopy. Journal of Physical Chemistry C, 2020, 124, 28061-28073.	1.5	20
130	Facet-Dependent selectivity of CeO2 nanoparticles in 2-Propanol conversion. Journal of Catalysis, 2021, 404, 96-108.	3.1	20
131	ZnAl <sub>2</sub> O <sub>4</sub> Spinel-Supported PdZn <sub>β</sub> Catalyst with Parts per Million Pd for Methanol Steam Reforming. ACS Catalysis, 2022, 12, 2714-2721.	5.5	20
132	Steam reforming of simulated bio-oil on K-Ni-Cu-Mg-Ce-O/Al2O3: The effect of K. Catalysis Today, 2019, 323, 183-190.	2.2	19
133	Surface engineering of earth-abundant Fe catalysts for selective hydrodeoxygenation of phenolics in liquid phase. Chemical Science, 2020, 11, 5874-5880.	3.7	19
134	Synergetic effect of Lewis acid and base in modified Sn-β on the direct conversion of levoglucosan to lactic acid. Catalysis Science and Technology, 2020, 10, 2986-2993.	2.1	19
135	Remarkable self-degradation of Cu/SAPO-34 selective catalytic reduction catalysts during storage at ambient conditions. Catalysis Today, 2021, 360, 367-374.	2.2	18
136	Elucidation of reaction mechanism for m-cresol hydrodeoxygenation over Fe based catalysts: A kinetic study. Catalysis Communications, 2017, 100, 43-47.	1.6	17
137	Oxidation of Methane to Methanol by Water Over Cu/SSZâ€┨3: Impact of Cu Loading and Formation of Active Sites. ChemCatChem, 2022, 14, .	1.8	17
138	Rate Controlling in Low-Temperature Standard NH <sub>3</sub> -SCR: Implications from <i>Operando</i> EPR Spectroscopy and Reaction Kinetics. Journal of the American Chemical Society, 2022, 144, 9734-9746.	6.6	17
139	Coverage-Dependent Adsorption of Hydrogen on Fe(100): Determining Catalytically Relevant Surface Structures via Lattice Gas Models. Journal of Physical Chemistry C, 2020, 124, 7254-7266.	1.5	15
140	Understanding the origin of selective oxidative dehydrogenation of propane on boron-based catalysis A: General, 2021, 623, 118271.	2.2	15
141	Deactivation by Potassium Accumulation on a Pt/TiO <sub>2</sub> Bifunctional Catalyst for Biomass Catalytic Fast Pyrolysis. ACS Catalysis, 2022, 12, 465-480.	5.5	15
142	Adsorption of aromatics on the (111) surface of PtM and PtM <sub>3</sub> (M = Fe, Ni) alloys. RSC Advances, 2015, 5, 85705-85719.	1.7	14
143	Adsorption and Reaction of Methanol on Anatase TiO <sub>2</sub> (101) Single Crystals and Faceted Nanoparticles. Journal of Physical Chemistry C, 2019, 123, 24133-24145.	1.5	14
144	Selective hydrogenolysis of aryl ether bond over Ru-Fe bimetallic catalyst. Catalysis Today, 2021, 365, 199-205.	2.2	14

#	Article	IF	CITATIONS
145	A Strategy for the Simultaneous Synthesis of Methallyl Alcohol and Diethyl Acetal with Snâ€Î². ChemSusChem, 2017, 10, 4715-4724.	3.6	13
146	Enhanced Antioxidation Stability of Iron-Based Catalysts via Surface Decoration with ppm Platinum. ACS Sustainable Chemistry and Engineering, 2018, 6, 14010-14016.	3.2	13
147	Noble Metal Singleâ€Atom Catalysts for the Catalytic Oxidation of Volatile Organic Compounds. ChemSusChem, 2022, 15, .	3.6	13
148	Surface Oxygen Vacancies Confined by Ferroelectric Polarization for Tunable CO Oxidation Kinetics. Advanced Materials, 2022, 34, e2202072.	11.1	13
149	Effect of Cobalt Particle Size on Acetone Steam Reforming. ChemCatChem, 2015, 7, 2932-2936.	1.8	12
150	Coverage-Dependent Adsorption of Phenol on Pt(111) from First Principles. Journal of Physical Chemistry C, 2020, 124, 356-362.	1.5	12
151	Propane ammoxidation over MoVTeNb oxide catalyst in a microchannel reactor. AICHE Journal, 2018, 64, 4002-4008.	1.8	11
152	Predicting the Electric Field Effect on the Lateral Interactions Between Adsorbates: O/Fe(100) from First Principles. Topics in Catalysis, 2018, 61, 763-775.	1.3	11
153	An Environmental Transmission Electron Microscopy Study of the Stability of the TiO <sub>2</sub> (1) Tj ETQq1	1 0.7843 1.5	14 rgBT /Ov
154	Understanding the Deactivation of Agâ^'ZrO <sub>2</sub> /SiO <sub>2</sub> Catalysts for the Singleâ€step Conversion of Ethanol to Butenes. ChemCatChem, 2021, 13, 999-1008.	1.8	11
155	The Effect of Pretreatment on the Reactivity of Pd/Al <sub>2</sub> O <sub>3</sub> in Room Temperature Formaldehyde Oxidation. ChemCatChem, 2021, 13, 4133-4141.	1.8	11
156	Oxidative esterification of acetol with methanol to methyl pyruvate over hydroxyapatite supported gold catalyst: Essential roles of acid-base properties. Chinese Journal of Catalysis, 2019, 40, 1810-1819.	6.9	10
157	Benchmarking the accuracy of coverage-dependent models: adsorption and desorption of benzene on Pt (1 1 1) and Pt3Sn (1 1 1) from first principles. Progress in Surface Science, 2019, 94, 100538.	3.8	10
158	Economizing on Precious Metals in Threeâ€Way Catalysts: Thermally Stable and Highly Active Singleâ€Atom Rhodium on Ceria for NO Abatement under Dry and Industrially Relevant Conditions**. Angewandte Chemie, 2021, 133, 395-402.	1.6	10
159	Conversion of Formic Acid on Single- and Nano-Crystalline Anatase TiO <sub>2</sub> (101). Journal of Physical Chemistry C, 2021, 125, 7686-7700.	1.5	10
160	Unveiling the Interfacial and Structural Heterogeneity of Ti <sub>3</sub> C <sub>2</sub> T <sub><i>x</i></sub> MXene Etched with CoF <sub>2</sub> /HCl by Integrated <i>in Situ</i> Thermal Analysis. ACS Applied Materials & Interfaces, 2021, 13, 52125-52133.	4.0	10
161	Thermal perturbation of NMR properties in small polar and non-polar molecules. Scientific Reports, 2020, 10, 6097.	1.6	9
162	Designing Ceria/Alumina for Efficient Trapping of Platinum Single Atoms. ACS Sustainable Chemistry and Engineering, 2022, 10, 7603-7612.	3.2	9

#	Article	IF	CITATIONS
163	Hierarchically structured catalysts for cascade and selective steam reforming/hydrodeoxygenation reactions. Chemical Communications, 2015, 51, 16617-16620.	2.2	8
164	Elucidating the Active Site and the Role of Alkali Metals in Selective Hydrodeoxygenation of Phenols over Ironâ€Carbideâ€based Catalyst. ChemSusChem, 2021, 14, 4546-4555.	3.6	8
165	Biomimetic CO oxidation below â^'100 °C by a nitrate-containing metal-free microporous system. Nature Communications, 2021, 12, 6033.	5.8	8
166	Stabilization and transformation of Pt nanocrystals supported on ZnAl2O4spinel. RSC Advances, 2017, 7, 3282-3286.	1.7	7
167	Hydrothermally stable ZnAl <sub>2</sub> O <sub>4</sub> nanocrystals with controlled surface structures for the design of long-lasting and highly active/selective PdZn catalysts. Green Chemistry, 2019, 21, 6574-6578.	4.6	7
168	Tailoring the Local Environment of Platinum in Singleâ€Atom Pt <sub>1</sub> /CeO <sub>2</sub> Catalysts for Robust Lowâ€Temperature CO Oxidation. Angewandte Chemie, 2021, 133, 26258-26266.	1.6	7
169	The partial reduction of clean and doped α-Fe2O3(0001) from first principles. Applied Catalysis A: General, 2019, 582, 116989.	2.2	6
170	Identifying the Thermal Decomposition Mechanism of Guaiacol on Pt(111): An Integrated X-ray Photoelectron Spectroscopy and Density Functional Theory Study. Journal of Physical Chemistry C, 2018, 122, 4261-4273.	1.5	5
171	Elucidating the Cooperative Roles of Water and Lewis Acid–Base Pairs in Cascade C–C Coupling and Self-Deoxygenation Reactions. Jacs Au, 2021, 1, 1471-1487.	3.6	5
172	High-Temperature and High-Pressure In situ Magic Angle Spinning Nuclear Magnetic Resonance Spectroscopy. Journal of Visualized Experiments, 2020, , .	0.2	5
173	Effects of high-temperature CeO <sub>2</sub> calcination on the activity of Pt/CeO <sub>2</sub> catalysts for oxidation of unburned hydrocarbon fuels. Catalysis Science and Technology, 2022, 12, 2462-2470.	2.1	5
174	Modeling the adsorbate coverage distribution over a multi-faceted catalytic grain in the presence of an electric field: O/Fe from first principles. Catalysis Today, 2018, 312, 92-104.	2.2	4
175	Critical Role of Al Pair Sites in Methane Oxidation to Methanol on Cu-Exchanged Mordenite Zeolites. Catalysts, 2021, 11, 751.	1.6	4
176	Noble Metal Singleâ€Atom Catalysts for the Catalytic Oxidation of Volatile Organic Compounds. ChemSusChem, 2022, 15, e202200356.	3.6	4
177	Guiding the design of oxidation-resistant Fe-based single atom alloy catalysts with insights from configurational space. Journal of Chemical Physics, 2021, 154, 174709.	1.2	3
178	Impact of Hydration on Supported V2O5/TiO2 Catalysts as Explored by Magnetic Resonance Spectroscopy. Journal of Physical Chemistry C, 2021, 125, 16766-16775.	1.5	3
179	Formation Energetics and Guest—Host Interactions of Molybdenum Carbide Confined in Zeolite Y. Industrial & Engineering Chemistry Research, 2021, 60, 13991-14003.	1.8	3
180	The effect of ZnO addition on H2O activation over Co/ZrO2 catalysts. Catalysis Today, 2016, 269, 140-147.	2.2	2

#	Article	IF	CITATIONS
181	Pd/FER vs Pd/SSZâ€13 Passive NOx Adsorbers: Adsorbateâ€controlled Location of Atomically Dispersed Pd(II) in FER Determines High Activity and Stability. Angewandte Chemie, 0, , .	1.6	2
182	Acetone to isobutene conversion on ZnxTiyOz: Effects of TiO2 facet. Journal of Catalysis, 2022, 410, 236-245.	3.1	2
183	Enhanced Selective Hydrogenolysis of Phenolic C–O Bonds over Graphene-Covered Fe–Co Alloy Catalysts. ACS Sustainable Chemistry and Engineering, 2022, 10, 8588-8596.	3.2	2
184	Reversible transformation between terrace and step sites of Pt nanoparticles on titanium under CO and O2 environments. Chinese Journal of Catalysis, 2022, 43, 2026-2033.	6.9	2
185	Hexagonal boron nitride for selective oxidative dehydrogenation of n-hexane to olefins. Applied Catalysis A: General, 2022, 643, 118763.	2.2	2
186	Frontispiece: Tailoring the Local Environment of Platinum in Singleâ€Atom Pt <sub>1</sub> /CeO <sub>2</sub> Catalysts for Robust Lowâ€Temperature CO Oxidation. Angewandte Chemie - International Edition, 2021, 60, .	7.2	1
187	Modelling complex molecular interactions in catalytic materials for energy storage and conversion in nuclear magnetic resonance. Frontiers in Catalysis, 0, 2, .	1.8	1
188	A Strategy for the Simultaneous Synthesis of Methallyl Alcohol and Diethyl Acetal with Sn-β. ChemSusChem, 2017, 10, 4667-4667.	3.6	0
189	Identifying Trends in the Field Ionization of Diatomic Molecules over Adsorbate Covered Pd(331) Surfaces. Topics in Catalysis, 2020, 63, 1510-1521.	1.3	0
190	Reply to: "Pitfalls in identifying active catalyst species― Nature Communications, 2020, 11, 4574.	5.8	0
191	Frontispiz: Tailoring the Local Environment of Platinum in Singleâ€Atom Pt <sub>1</sub> /CeO <sub>2</sub> Catalysts for Robust Lowâ€Temperature CO Oxidation. Angewandte Chemie 2021 133	1.6	0